NAVAL POSTGRADUATE SCHOOL

MONTEREY, CALIFORNIA

THESIS

DYNAMIC FAILURE OF SANDWICH BEAMS WITH FLUID-STRUCTURE INTERACTION UNDER IMPACT LOADING

by

Ryan D. McCrillis

December 2010

Thesis Advisor:	Young W. Kwon
Second Reader:	Jarema M. Didoszak

Approved for public release; distribution is unlimited

THIS PAGE INTENTIONALLY LEFT BLANK

REPORT DOCUMENTATION PAGE			Form Approved OMB No. 0704-0188

Public reporting burden for this collection of information is estimated to average 1 hour per response, including the time for reviewing instruction, searching existing data sources, gathering and maintaining the data needed, and completing and reviewing the collection of information. Send comments regarding this burden estimate or any other aspect of this collection of information, including suggestions for reducing this burden, to Washington headquarters Services, Directorate for Information Operations and Reports, 1215 Jefferson Davis Highway, Suite 1204, Arlington, VA 22202-4302, and to the Office of Management and Budget, Paperwork Reduction Project (0704-0188) Washington DC 20503.

1. AGENCY USE ONLY *(Leave blank)*	2. REPORT DATE December 2010	3. REPORT TYPE AND DATES COVERED Master's Thesis

4. TITLE AND SUBTITLE Dynamic Failure of Sandwich Beams With Fluid-Structure Interaction Under Impact Loading	5. FUNDING NUMBERS
6. AUTHOR(S) Ryan McCrillis	
7. PERFORMING ORGANIZATION NAME(S) AND ADDRESS(ES) Naval Postgraduate School Monterey, CA 93943-5000	8. PERFORMING ORGANIZATION REPORT NUMBER
9. SPONSORING /MONITORING AGENCY NAME(S) AND ADDRESS(ES) N/A	10. SPONSORING/MONITORING AGENCY REPORT NUMBER

11. SUPPLEMENTARY NOTES The views expressed in this thesis are those of the author and do not reflect the official policy or position of the Department of Defense or the U.S. Government. IRB Protocol number: N/A.

12a. DISTRIBUTION / AVAILABILITY STATEMENT Approved for public release; distribution is unlimited.	12b. DISTRIBUTION CODE

13. ABSTRACT (maximum 200 words)

The objective of this research is to examine the added mass effect that water has on the dynamic response of a sandwich composite under impact, particularly impact leading to failure. Because sandwich composites are much less dense than water, fluid structure interaction plays a large part in the failure. Composite samples were constructed using vacuum assisted transfer molding, with a 6.35 mm balsa core and symmetrical plain weave 6 oz E-glass skins. The experiment consisted of three phases. First, using three-point bending, strain rate characteristics were examined both in air and under water. After establishing that the medium had no effect on the beam response under different strain rates, but confirming that previously established relationships between strain rate and ultimate strength for axially loaded glass composites can be applies to sandwich construction in bending, the experiment progressed to impact testing where each specimen, again a one inch wide beam, was subjected to progressively increasing force. The data from this phase showed that submerged samples failed at lower drop heights and lower peak forces with a failure mode dominated by center span skin compression failure. Beams in air were able to withstand higher drop heights and peak forces. Dry sample failure mode was dominated by skin compression failure at the clamped support with occasional evidence of shear failure through the core adjacent to the clamped support. The data from this study will increase understanding of sandwich composite characteristics subjected to underwater impact.

14. SUBJECT TERMS Sandwich Composite, Low Velocity Impact, Submerged, Fluid-structure Interaction			15. NUMBER OF PAGES 57
			16. PRICE CODE
17. SECURITY CLASSIFICATION OF REPORT Unclassified	18. SECURITY CLASSIFICATION OF THIS PAGE Unclassified	19. SECURITY CLASSIFICATION OF ABSTRACT Unclassified	20. LIMITATION OF ABSTRACT UU

NSN 7540-01-280-5500

Standard Form 298 (Rev. 2-89)
Prescribed by ANSI Std. 239-18

THIS PAGE INTENTIONALLY LEFT BLANK

Approved for public release; distribution is unlimited

DYNAMIC FAILURE OF SANDWICH BEAMS WITH FLUID-STRUCTURE INTERACTION UNDER IMPACT LOADING

Ryan D. McCrillis
Lieutenant Commander, United States Navy
B.S., U.S. Naval Academy, 1998

Submitted in partial fulfillment of the
requirements for the degree of

MASTER OF SCIENCE IN MECHANICAL ENGINEERING

from the

NAVAL POSTGRADUATE SCHOOL
December 2010

Author: Ryan D. McCrillis

Approved by: Young W. Kwon
Thesis Advisor

Jarema M. Didoszak
Second Reader

Knox T. Millsaps
Chairman, Department of Mechanical and Aerospace Engineering

THIS PAGE INTENTIONALLY LEFT BLANK

ABSTRACT

The objective of this research is to examine the added mass effect that water has on the dynamic response of a sandwich composite under impact, particularly impact leading to failure. Because sandwich composites are much less dense than water, fluid structure interaction plays a large part in the failure. Composite samples were constructed using vacuum assisted transfer molding, with a 6.35 mm balsa core and symmetrical plain weave 6 oz E-glass skins. The experiment consisted of three phases. First, using three-point bending, strain rate characteristics were examined both in air and under water. After establishing that the medium had no effect on the beam response under different strain rates, but confirming that previously established relationships between strain rate and ultimate strength for axially loaded glass composites can be applies to sandwich construction in bending, the experiment progressed to impact testing where each specimen, again a one inch wide beam, was subjected to progressively increasing force. The data from this phase showed that submerged samples failed at lower drop heights and lower peak forces with a failure mode dominated by center span skin compression failure. Beams in air were able to withstand higher drop heights and peak forces. Dry sample failure mode was dominated by skin compression failure at the clamped support with occasional evidence of shear failure through the core adjacent to the clamped support. The data from this study will increase understanding of sandwich composite characteristics subjected to underwater impact.

THIS PAGE INTENTIONALLY LEFT BLANK

TABLE OF CONTENTS

I. INTRODUCTION 1
- **A. BACKGROUND 1**
- **B. LITERATURE SURVEY 2**
  - **1. Impact Effect on Composites 2**
  - **2. Strain Rate Effect on Composites 3**
- **C. OBJECTIVES 4**

II. COMPOSITE CONSTRUCTION AND METHODOLOGY 5
- **A. COMPOSITE CONSTRUCTION 5**
  - **1. Material and Chemical Requirements 6**
  - **2. Chemical Composition of the Resin Matrix 6**
  - **3. Layup Procedures 7**
  - **4. Coupon Preparation 10**
  - **5. Strain Gages 10**
- **B. MATERIAL SELECTION AND PROPERTIES 12**
  - **1. E-glass 12**
  - **2. Balsa 12**
- **C. TESTING EQUIPMENT 13**
  - **1. Three Point Bending 13**
    - ***a. MTS Machine 13***
    - ***b. Three Point Bending Fixture 14***
    - ***c. Submersion Tank 14***
    - ***d. Data Acquisition 15***
  - **2. Impact Testing 15**

III. RESULTS AND DISCUSSION 19
- **A. OVERVIEW 19**
- **B. THREE POINT BENDING 20**
- **C. IMPACT TESTING 21**
- **D. STRAIN DATA 27**
- **E. DISCUSSION 32**
  - **1. Failure Mode 32**
  - **2. Failure Loads and Drop Height 33**

IV. CONCLUSIONS AND RECOMMENDATIONS 35

LIST OF REFERENCES 37

INITIAL DISTRIBUTION LIST 39

THIS PAGE INTENTIONALLY LEFT BLANK

LIST OF FIGURES

Figure 1. VARTM setup (After Owens) 5
Figure 2. Dry layup, bottom to top: Teflon, distribution medium, peel ply, E-glass, Balsa Core, E-glass. Not yet added: peel ply, distribution medium, vacuum film. 8
Figure 3. Resin flowing through the layup.....9
Figure 4. Strain gage placement (Unit in inches followed by millimeters in parentheses).....11
Figure 5. Strain gage placement on dry layup.....11
Figure 6. Three-point bending fixture 14
Figure 7. Piezo electric load cell 16
Figure 8. Failure force verses crosshead speed (untreated balsa) 21
Figure 9. Medium has no effect of failure load but increasing strain rate increases ultimate strength. (hot coated balsa) 21
Figure 10. Dry Balsa with no damage.....24
Figure 11. Dry Balsa Failure 25
Figure 12. Dry impact damage with core shearing. The rightmost fracture line was right at the edged of the clamped boundary. 25
Figure 13. Submerged impact without failure.....26
Figure 14. Submerge impact failure. 27
Figure 15. Typical submerged impact damage. 27
Figure 16. Dry impact, centerline and boundary failure 29
Figure 17. Submerged impact, centerline failure 29
Figure 18. Submerged impact, no failure.....30
Figure 19. Submerged impact, mid-span failure 30
Figure 20. Submerged impact, boundary failure.....31
Figure 21. Submerged impact, boundary and mid-span failure 31
Figure 22. Shear force diagram 33
Figure 23. Bending moment diagram.....33

THIS PAGE INTENTIONALLY LEFT BLANK

LIST OF TABLES

Table 1. Comparison of experimental results on the effect of strain rate on the mechanical properties of glass composites. (After Tan).....4
Table 2. Table 1 Resin Matrix Composition by volume.....6
Table 3. E-glass/Vinyl-Ester Material Properties, after Owens[2]. 12
Table 4. Material Properties of ProBalsa Plus™, ...13
Table 5. Failure locations.....22
Table 6. Progressive impact data 23
Table 7. Single drop impact data 23
Table 8. Average force for equal impact velocity.....34

THIS PAGE INTENTIONALLY LEFT BLANK

EXECUTIVE SUMMARY

The objective of this research is to examine the added mass effect that water has on the dynamic response of a sandwich composite under impact, particularly impact leading to failure. Because sandwich composites are much less dense than water, the fluid structure interaction plays a large part in the failure. Composite samples were constructed using vacuum assisted transfer molding, with a 6.35 mm balsa core and symmetrical plain weave 6 oz E-glass skins. The experiment consisted of three phases. First, using three-point bending, strain rate characteristics were examined in both air and under water. After the establishing that the medium had no effect on the beam response under different strain rates, but confirming that previously established relationships between strain rate and ultimate strength for axially loaded glass composites can be applied to sandwich construction in bending, the experiment progressed to impact testing where each specimen, again a one inch beam, was subjected to progressively increasing force. The data from this phase showed that submerged samples failed at lower drop heights and lower peak forces with a failure mode dominated by center span skin compression failure. Beams in air were able to withstand higher drop heights and peak forces. Dry sample failure mode was dominated by compression failure at the boundary. The data from this study will increase understanding of cored composite characteristics subjected to underwater impact.

THIS PAGE INTENTIONALLY LEFT BLANK

ACKNOWLEDGMENTS

I would like thank my wife and family for their encouragement and support throughout the thesis process. I am also very grateful to Dr. Kwon and Tom Christian for their patience, wisdom and guidance. John Mobley and Jason Brunton were invaluable in construction and utilization of the test gear. In addition, I owe a debt of gratitude to my good friend Todd Green who inspired me to transition to Engineering Duty. Above all, I thank God for putting all these people in my life and giving me the vision for this project.

THIS PAGE INTENTIONALLY LEFT BLANK

I. INTRODUCTION

A. BACKGROUND

Composite construction is oft lauded for its ability to deliver high stiffness and strength with low weight. It is extremely useful in applications ranging from advanced aerospace designs to low cost recreational equipment. The most common form of composite construction entails use of continuous fibers such as E-glass, S-Glass, Carbon, Kevlar, and many other suitable fibers, often woven into a cloth, reinforced and held in matrix with various types of resins. Both strength and stiffness for bending loads increase as a function of the bending stiffness. Larger bending stiffness are achieved without adding significant weight by creating a sandwich structure consisting of a low density core bonded with a reinforced fiber skin.

Core selection is based on a variety of requirements, such as cost, density and strength, bonding strength, and even fire resistance. Foam, both closed and open celled, honeycomb structures, and wood are all popular choices, with end grain balsa being one of the most common choices for marine construction due to its high compressive strength, good bonding properties and low cost [1].

There are many different failure modes for a sandwich composite. A common failure in a marine environment is delamination caused by water intrusion. Delamination drastically reduces the composite's stiffness and strength. In bending, the outer skin can fail in tension, the inner skin can fail in compression, the core can experience a shear failure, and the upper skin can de-bond from the core. Localized impact can cause punch through, where the core is deformed directly beneath the impact. Impact can also cause delamination in any part of the composite. Due to the fact that most fibers are stronger in tension than compression, compression failure at the skin is commonly the beginning of a failure sequence that can include all of the previously mentioned failure modes.

Damage caused by impact is further complicated by several issues. Denting of the skin results in a stress concentration around the impact area do to change in geometry, further reducing the strength of skin in compression. High strain rates can often affect

the properties of the composite material and the added mass of the water medium in which the composite is responding will affect impact response significantly. The fluid/structure interaction that takes place as part of the dynamic response is of particular interest for marine applications.

In previous experiments, Kwon and Owens [2] observed an increased amplitude response when a carbon plate was impacted under water. It was conjectured that this effect may have been due to an added mass phenomenon, since the carbon plate was only slightly denser than the water it was in. With a sandwich structure, the cored composite is much less dense water, suggesting that added mass will have an even more profound effect on dynamic response.

Because composites are being used more and more frequently in underwater structures such as submarine sails, sonar domes, rudders, and even propellers, as well as hull skin and structure, there is a need to understand composite characteristics in order to successfully design such structures [3]. Impact damage is a serious design concern because composite structures are more susceptible to impact damage than similar metallic structures. Not only are they typically not as hard, but they also lack the ductility that allows metallic structures to absorb large amounts of energy without failure [4]. In addition, the damage in composites from impact can go undetected, even when the mechanical properties may be drastically reduced by impact damage. For these reasons, numerous experimental and analytical studies have been conducted to study the dynamic response of composites subjected to transient dynamic loading.

B. LITERATURE SURVEY

1. Impact Effect on Composites

In 1994, Abrate [5] reviewed over 300 articles on the current advances on impact on laminated composites to provide a comprehensive view of the state of knowledge in the area. The predominance of this research is focused on low velocity impact damage, focusing on damage predictions and evaluation of residual properties of

damaged laminates. The entire body of this research is on composites under low velocity impact in dry surroundings, mainly to support development of composites for aircraft structures.

Recently, however, some new work has started looking at fluid composite structure interaction with composites under low velocity impact. In 2009, Hampson and Moatamedi [6] found that unidirectional carbon composite plates underwent smaller accelerations and experienced less damage when impacted underwater.

2. Strain Rate Effect on Composites

There have been many investigations into the relationship between strain rate and the material properties of composites. Due to the unique characteristics of a composite based on resin, reinforcing fiber material, fiber orientation, it is difficult to draw a complete picture of the effect of strain rate across the board. In attempting to make a fair comparison, only studies examining glass fiber composites will be cited.

Tan [7] summarized the following:

Armenakas and Sciammarella [8] established that the dynamic elastic modulus varies linearly with the logarithm of the strain rate and Lifshitz [9] showed dynamic failure stresses were noticeably higher than the corresponding static values while failure strains and moduli were unaffected by the rate of loading in glass/epoxy laminates.

In another study on the effects of the strain rate, Okoli [10] carried out tensile, shear and three-point bend tests on a woven glass/epoxy laminate and established a linear relationship between expended energy and the logarithm of the strain rate. Shokrieh and Omidi [11] supported this in unidirectional glass fiber reinforced polymeric composites under uniaxial loading at quasi-static and intermediate strain rates. They also noted that failure changed from quasi-static to high dynamic loading conditions.

Table 1 summarizes the results of some of the studies done in this area. It is noted that several of the above studies suggested linear relationships between the logarithm of strain rate and various material characteristics including dynamic elastic modulus, yield stress and expended energy.

Table 1. Comparison of experimental results on the effect of strain rate on the mechanical properties of glass composites. (After Tan)

Study by	Composite	Effect of increasing strain rate on			
		Ultimate tensile strength	Modulus	Failure strain	Other characteristics
Armenakas and Sciammarella [8]	Glass/epoxy	Decrease	Increase	Decrease	-
Lifshitz [9]	Angle ply glass/epoxy	Increase	Independent	Independent	-
Daniel *et al.* [12]	Carbon/epoxy	Independent	Increase slightly	Independent	-
Harding and Welsh [13]	Glass/epoxy	Increase	Increase	Increase	Absorbed failure energy increases
	Carbon/epoxy	Independent	Independent	-	-
Okoli and Smith [14]	Glass/epoxy	Increase	Increase	-	Poisson's ratio independent
Shokrieh and Omidi [11]	Glass/epoxy	Increase	Increase slightly	Increase slightly	Absorbed failure energy increases

C. OBJECTIVES

The goal of this study is to understand and analyze the effect that added mass has on impact failure of a balsa-cored sandwich composite under low velocity impact. The data gathered should increase understanding of fluid structure interaction in general and sandwich composite failure modes in particular.

II. COMPOSITE CONSTRUCTION AND METHODOLOGY

A. COMPOSITE CONSTRUCTION

The composite test panels were constructed to match, as closely as possible, the industry standard used in today's marine construction. The test panels were constructed using a vacuum assisted resin infusion process (VARTM) shown in Figure 1.

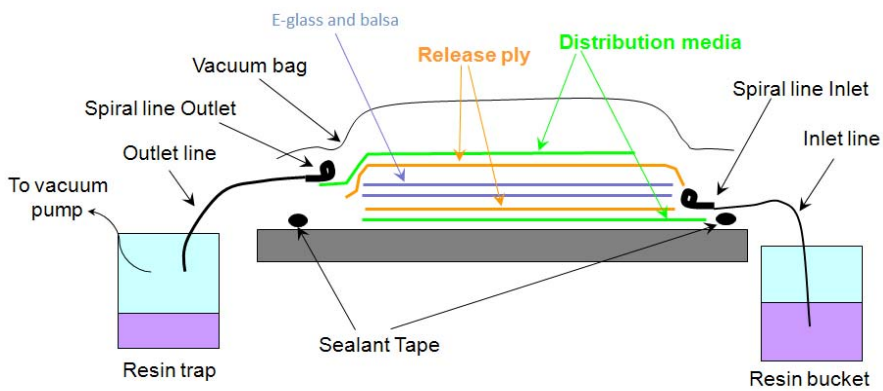

Figure 1. VARTM setup (After Owens)

Each composite consists of a 6.35 mm end grain balsa core with skin consisting of 2 or 3 layers of non-biased, plain weave 6 oz E-glass laid at 0/90 degree orientation. As the experiment progressed, it was obvious that the non homogenous nature of the balsa caused unequal resin absorption resulting in resin starvation at some spots in the panel. These flaws, as well as naturally occurring internal anomalies such as sap lines and knots, caused a great deal of data scatter. To combat this problem, balsa was treated with a thin "hot coat" of highly catalyzed resin. This produced much tighter results, but still provided a lot of room for variability in construction. Panels were finally constructed from ProBalsa Plus, an industrial core material from DIAB with a density of 155 kg/m^3 ProBalsa Plus is micro sanded and treated with a special coating to reduce resin absorption.

1. Material and Chemical Requirements

The material and chemical requirements necessary to mimic standard maritime construction techniques consisted of Derakane 510A vinyl ester resin, Methyl Ethyl Ketone Peroxide (MEKP), Cobalt Naphthenate (CoNap), Ndimthylaniline (DMA), and 5.8 oz/square yard plain weave E-glass cloth. In addition to the composite ingredients, fabrication required glass plates, peel ply, Airtech® Resinflow 75 distribution medium, Stretchlon 200 1.5 vacuum bag film, AT-200Y sealant tape, spiral wrap, vacuum hose, and a vacuum pump. The glass plates were used as a foundation for building the composite pieces. Prior to layup, the glass was waxed with high temp mold release wax to aid in removal of the finished panel. Distribution medium assisted resin flow on both sides of the core and peel ply was used to prevent the resin from sticking to the distribution medium. Resin was drawn into the sample through the spiral wrap which allowed even flow across the entire sample. On the vacuum side, spiral wrap was used to create even vacuum across the sample. Excess resin was drawn through the back spiral wrap, through vacuum tubing and into a resin trap.

2. Chemical Composition of the Resin Matrix

Derakane 510A was used as the base matrix resin throughout the project. MEKP, CoNap, and DMA were used as hardening and accelerating agents, with amounts varied to achieve the desired gel time of 45 minutes. Normal ambient temperature in the lab remained between 17° C and 20° C. To achieve a gel time of approximately 45 minutes, the ratios in Table 2 were followed.

Table 2. Table 1 Resin Matrix Composition by volume

Component	Amount
DERAKANE 510-A	1000 mL
Methyl Ethyl Ketone Peroxide (MEKP)	12.5 mL
Cobalt Napthenate (CoNAP)	3 mL
N, N- Dimethylaniline (DMA)	.5 mL

3. Layup Procedures

Once the proper procedure for composite construction was identified, the procedure was standardized to ensure each test sample was constructed in the same fashion. Each sample consisted of 2 or 3 plies of E-glass sandwiching a 6.35 mm balsa core. The step by step process has been articulated and illustrated below.

Step 1: Cut balsa core: desired size

Cut 6 sheets E-glass fabric: desired size

Cut 3 sheets of peel ply: 5 cm larger than fabric and core

Cut 2 sheets of distribution medium: same size as peel ply

Cut 1 sheet of vacuum film: 10 cm larger than peel ply.

Step 2: Tape edges of glass plate with continuous line of sealant tape. Do not remove backing.

Step 3: Wax glass or lay out Teflon sheets inside taped area to facilitate mold release.

Step 4: Layup material in the following order from bottom to top: distribution medium (required on mold side since skin thickness limits resin flow), peel ply, 3 sheets of E-glass, fibers aligned, balsa core, 3 sheets of E-glass, peel ply, distribution medium, peel ply (to protect the vacuum film from the cut edges of the distribution medium.) Figure 2 shows the beginning of this layup sequence.

Figure 2. Dry layup, bottom to top: Teflon, distribution medium, peel ply, E-glass, Balsa Core, E-glass. Not yet added: peel ply, distribution medium, vacuum film.

Step 5: Route feed hose and suction hose to the layup and wrap with sealant tape where they cross the tape line on the glass.

Step 6: Cut 2 pieces of spiral wrap approx 30in each (the length of the sample) and insert one end of each into the feed and suction hoses respectively. Lay the spiral wrap along the edge of the panel, taking care that is in contact with the distribution medium at every point. A small piece of sealant tape can help hold it in place.

Step 7: Remove the tape backing and apply the vacuum film over the entire layup. Ensure good adhesion between the film and tape.

Step 8: With the feed hose plugged, draw a vacuum to de-bulk the material and check for leaks. Hold the vacuum from this point on. There are several possible techniques to plug the hose, but one of the most effective is sticking the feed hose into a small amount of used sealant tape on the bottom of the feed container. This facilitates starting resin flow without allowing excess air back into the layup.

Step 9: Combine chemicals in the order shown below and stir continuously.

2 L Derakane 510A, 6 mL CoNp, 1 mL DMA

Mix thoroughly prior to addition of MEKP as accelerates and hardener can have a violent exothermic reaction if allowed in direct contact.

Add 25mL MEKP.

Allow 10-15 minutes for resin to gas off. Resin should be a uniform amber color with no bubbles prior to infusion.

Step 10: Pour mixed resin into feed container and break the feed hose seal. Resin will be drawn through the feed hose, into the spiral wrap and across the sample as shown in Figure 3. Check for air leaks and plug them with extra sealant tape.

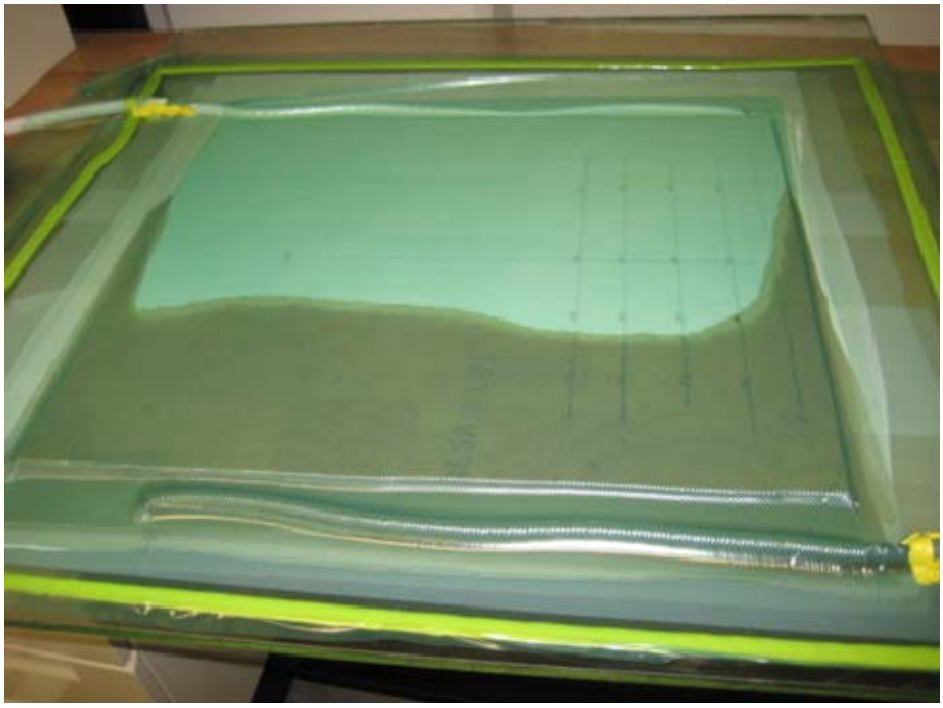

Figure 3. Resin flowing through the layup

Step 11: Once the layup is fully infused, stop by bending the feed hose and clamping it while keeping the end beneath the surface of the resin in the feed bucket.

Pray that it does not leak. It may be necessary to add more resin to keep the end of the feed tube submerged. Infusion should take 10-15 minutes, depending on resin viscosity, a function of resin temperature.

Step 8: After eight hours of curing, turn off the vacuum. Remove film, peel ply and distribution medium.

The composite plate is now ready for coupon preparation.

4. Coupon Preparation

Coupons were cut with a high quality laminate blade on a table saw with 80 teeth per inch. Dimensions for the three point bending phase were 178.8 (7 in) x 25.4 mm (1 in) for a 152.3 mm (6 in) test span. The coupons for impact testing were 457.2 (18 in) x 25.4 mm (1 in) for a 304.8 mm (12 in) test span. The dimensions were chosen to ensure that the coupon would fail under 10 kN force in three point bending.

Both sides of the coupon where core is exposed were waxed with mold release wax to inhibit water intrusion into the core.

5. Strain Gages

A small number of coupons were prepared with uni-directional strain gages as part of the layup as shown in figure 4. This application technique showed good adhesion and resilience through multiple impacts. It also had the advantage of placing the gages directly on top of the outer ply of E-glass rather than attempting to glue the gage to the outer resin layer that has taken the shape of the peel ply weave. One of the drawbacks to this technique is the difficulty in maintaining alignment during the dry layup. Once the vacuum is drawn, however, flowing resin does not appear to displace the gages.

Strain gages were placed at mid span, quarter span, eighth span, and on the free side of the clamped support boundary as depicted in Figures 4 and 5.

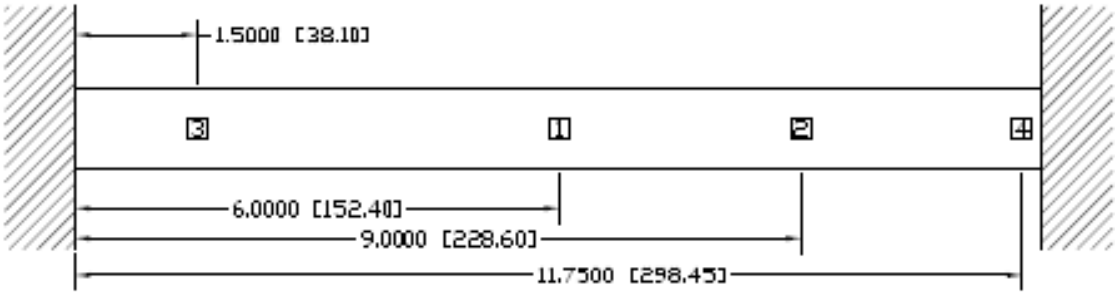

Figure 4. Strain gage placement (Unit in inches followed by millimeters in parentheses)

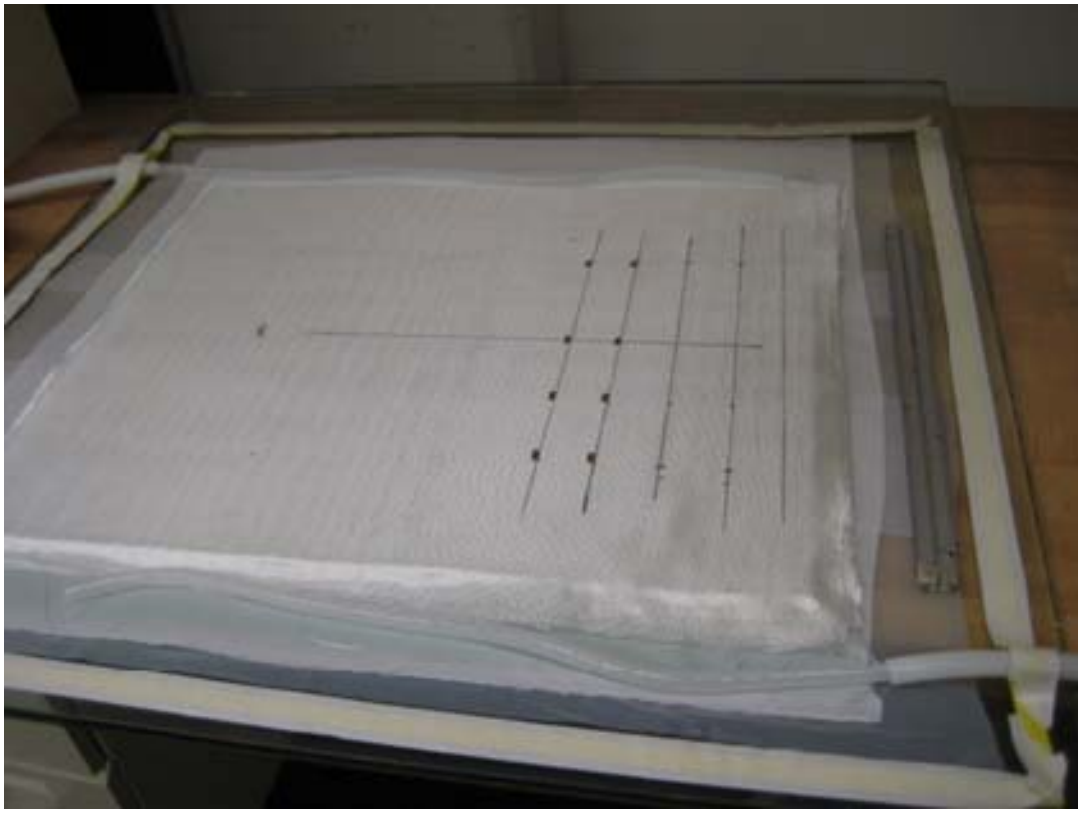

Figure 5. Strain gage placement on dry layup

B. MATERIAL SELECTION AND PROPERTIES

1. E-glass

Skin material for this study was 5.8 oz/square yard non-biased plain weave E-glass cloth. All plies were laid 0, 90 so 50% of the fibers were oriented along the length of the coupon with the other 50% oriented across the coupon to simplify analysis. E-glass has a wide range of published properties, but with an average tensile strength of 3.45 GPA it was ideal for keeping coupon breaking forces less than the 10KN limit of the load cell. E-glass also has the added advantage of being somewhat translucent, making damage analysis more accurate. Table 3 describes the characteristics of E-glass in matrix with Vinyl-Ester such as Derakane 510A.

Table 3. E-glass/Vinyl-Ester Material Properties, after Owens[2].

E-glass/Vinyl-Ester Composite

Density	2020	Kg/m3
E_{xt}	17.24×10^9	Pa
E_{yt}	17.24×10^9	Pa
E_z	7.929×10^9	Pa
G_{xy}	6.619×19^9	Pa
G_{xz}	2.896×19^9	Pa
G_{yz}	2.896×19^9	Pa
v_{xy}	0.3	
v_{xz}	0.24	
v_{yz}	0.24	

2. Balsa

End grain balsa core material is composed of square sections of cross cut balsa glued together much like a butcher block. With the grain oriented vertically, the cellular structure of the balsa wood is often characterized as micro honeycomb structure. This structure has very good properties in both compression and shear. Furthermore, because it is a naturally occurring, rapidly renewable resource, it is relatively inexpensive [16].

This ideal core material is very popular in the maritime industry, and, in fact, is used in many naval applications. Table 4 summarizes the primary characteristics of DIAB's ProBalsa Plus™.

Table 4. Material Properties of ProBalsa Plus™,

TECHNICAL DATA - TABLES

CHARACTERISTICS – PB

Property	Unit	Value	Test Procedure
Density	kg/m³ lb/ft³	155 9.7	ASTM C 271
Minimum Density	kg/m³ lb/ft³	121 7.6	ASTM C 271
Compressive Strength	MPa psi	12.7 1,841	ASTM C 365
Minimum Compressive Strength	MPa psi	6.4 928	ASTM C 365
Compressive Modulus	MPa psi	4,100 594,500	ASTM C 365
Minimum Compressive Modulus	MPa psi	2,000 290,000	ASTM C 365
Tensile Strength	MPa psi	13.5 1,957	ASTM C 297
Minimum Tensile Strength	MPa psi	7.5 1,087	ASTM C 297
Shear Strength	MPa psi	3.0 435	ASTM C 273
Minimum Shear Strength	MPa psi	1.8 261	ASTM C 273
Shear Modulus	MPa psi	166 24,070	ASTM C 273
Minimum Shear Modulus	MPa psi	100 14,500	ASTM C 273
Thermal Conductivity 23°C	W/(m · °C) Btu · in/(ft² · h · °F)	0.064 0.44	ASTM C 177
Moisture Content	%	12	ASTM D 2016
Minimum Moisture Content	%	8	ASTM D 2016
Water Absorption 24 hours 48 hours Saturation	%	225 310 625	ASTM C 272

PROBALSA

C. TESTING EQUIPMENT

1. Three Point Bending

Three point bending was conducted on an MTS Machine using a specially designed three point bending fixture and submersion tank.

a. MTS Machine

The MTS universal test machine is hydraulically operated and capable of precise crosshead movement controlled by customized programs in Station Manager.

Hydraulic wedge grips facilitate alignment and consistency. For this series of testing a program was created to allow manual selection of crosshead speed. Crosshead movement was program to stop after 15 mm of motion to prevent damage to the machine. This was sufficient deflection to cause failure in all coupons.

b. Three Point Bending Fixture

This stainless steel fixture was constructed in the NPS machine shop with a span of 152.4 mm (6 in) and a depth of 50.8 mm (2 in) to conduct testing in accordance with ASTM D 709 [17]. The fixture was attached to the hydraulic grips via a squared stud threaded into a hole tapped in the center of the bottom of the fixture. The 50.8 mm (2 in) wide center point is composed of 6.35 (0.25 in) mm aluminum stock with a radius milled along the contact edge. Figure 6 shows the fixture with coupon in place in the submersion tank.

Figure 6. Three-point bending fixture

c. Submersion Tank

A tank was constructed of 6.38 mm (.25 in) acrylic sheets fusion welded and sealed with 3M 5200. It measures 254 mm (10 in) by 431.8 mm (17 in) by 228.6 mm (9 in). The tank contains approximately 18.9 L (5 gal) of water to achieve a specimen depth of 50.8 mm (2 in) below the free surface. A ball valve attached to a standard garden hose can drain the tank in 5 minutes.

d. Data Acquisition

The MTS universal test machine is controlled by Test Star ™ IIs Station Manager Version 3.3B software. This program also manages data acquisition and storage. Data for this procedure was taken on two channels, one for force from the 10 kN force gage, and one for displacement

2. Impact Testing

Impact tests were conducted using a specially designed drop weight instrumented testing system thoroughly described by Owens [15] that consisted of a drop weight impactor, load transducer, strain gages, high speed data analyzer,. The machine was modified slightly to decrease the gap between the force gage and the specimen in order to achieve greater throw and ensure specimen failure. A new force gage with an axial connecter was also fitted to the machine to prevent connector damage in the event that the force gage penetrated the specimen. As in Owens' experiment, 76 mm (3 in) C-clamps were used to facilitate clamped boundary conditions, but with 25.4 mm (1 in) wide beams rather than plates. Transient response of the sample included load and strain as a function of time.

During testing, the impact tower was lowered into a well that could be filled with water, so that the submerged samples were 177.8 mm (7 in) below the free surface. Dry testing took place with the tower in the same position, but with the water level in the well lowered in order to maintain similar boundary conditions between tests. a. Load Transducer

The load cell was an ICP® force sensor manufactured by PCB Piezotronics, Inc., which converts force into a measurable electrical output. The load transducer was mounted on the end of the impactor rod, as shown in Figure 7. The gage had a diameter of 16mm. In order to increase longevity in an aqueous environment, both the gage and cable connection were coated with M coat A bond. Additional waterproofing was provided by a thin latex sleeve fitted over the end of the impacting rod.

Figure 7. Piezo electric load cell

As with Owen's experiment, data acquisition was carried out using a specifically developed acquisition system that consisted of a Pentium™ 4, 2.4 GHz, 512-MB RAM system, National Instruments™ simultaneous sampling multifunction DAQ, and five Vishay™ 2120 multi-channel strain signal conditioners. The system had a 16-bit analog-to-digital conversion resolution and was capable of reading a total of 16 channels at a

throughput rate of up to 250 kS/s per channel, Data was recorded at 10,000 Hz for 100 milliseconds each time the trigger was activated. The data-acquisition process was controlled using the NI-DAQmx driver software and LabVIEW™ interactive data-logging software that was specifically formatted at the Naval Postgraduate School for this research [15]. A trigger located on the drop weight was used to initiate data acquisition. Errors due to instrumentation noise did not seem to cause problems in the data, so no filtering was used. However, max voltage spikes were manually removed from the data during post processing.

THIS PAGE INTENTIONALLY LEFT BLANK

III. RESULTS AND DISCUSSION

A. OVERVIEW

Dealing with a sandwich composite greatly increases the number of variables that can affect the outcome of a test. This is particularly true when using a material produced in nature like balsa wood. Natural flaws and discontinuities affect not only peak strengths, but also modes of failure. Consequently, there is more scatter in the data than desired. However, even with this scatter, some distinct trends can be observed.

As the experiment progressed, the following changes were made to improve consistency: Balsa core was hot coated, that is, coated with a thin layer of highly activated resin that hardened quickly before being absorbed, prior to layup and infusion. This significantly reduced resin starvation in the more porous sections of the core, but still left room for deviation due to manual application of the hot coat. Following one lay up with this technique; the core material was again upgraded to ProBalsa Plus™, a product that has already been treated with a similar procedure in the factory. Because of the changes in construction procedure, comparative data is only valid when comparing coupons cut from the same panel.

As the experiment moved into higher strain rates and impact speeds, some localized indentation was observed. To prevent this from becoming the primary failure mode, the skin thickness was increase from two plies of 6 oz E-glass to three. With this skin thickness, there was no localized indentation in any specimen.

Because each phase of this study was conducted both wet and dry, the edged of every coupon, anywhere core material was exposed, was waxed with mold release wax to prevent water intrusion. This method of protection proved to be sufficient for the immersion times in this experiment.

The types of failure observed during this study were:

1. Delamination-Skin is separated from the core.

2. Skin compression-Core intact, but able to be compressed longitudinally in the vicinity of the failure if the fractured coupon is bent with the crack on the inside of the bend. Delamination may occur adjacent to the compression crack.

3. Shear failure-Core is fractured across the vertical cellular structure. Core is fractured vertically with delamination of upper and lower skin, often on opposite sides of the crack.

4. Core compression-Local indentation causing cellular columns of the balsa to collapse.

B. THREE POINT BENDING

Over 100 samples were tested using ASTM method D 709 for three point bending [17]. Strain rates were varied from sample to sample, but remained constant for any one test. Strain rate is assumed to be proportional to crosshead speed based on the equation for stress at the outer fiber where displacement is replaced by velocity [18]. Failure always occurred on the top surface at or near centerline. Mode of failure was skin compression, occasionally accompanied by local indentation. Delamination was occasionally seen, particularly at high strain rates. Data showed significant scatter due to inconsistencies in the balsa core and no correlation could be established between wet and dry samples (Figure 8). However, there was a general strengthening trend with increased crosshead speed, which is consistent with previous findings. A final test using hot coated balsa at two strain rates, one high and one low (Figure 9), had much tighter grouping with no outliers. This test supported the trend observed in previous tests and was judged conclusive that water medium did not affect the stress strain curve under a constant strain rate, i.e., without the inertia effect.

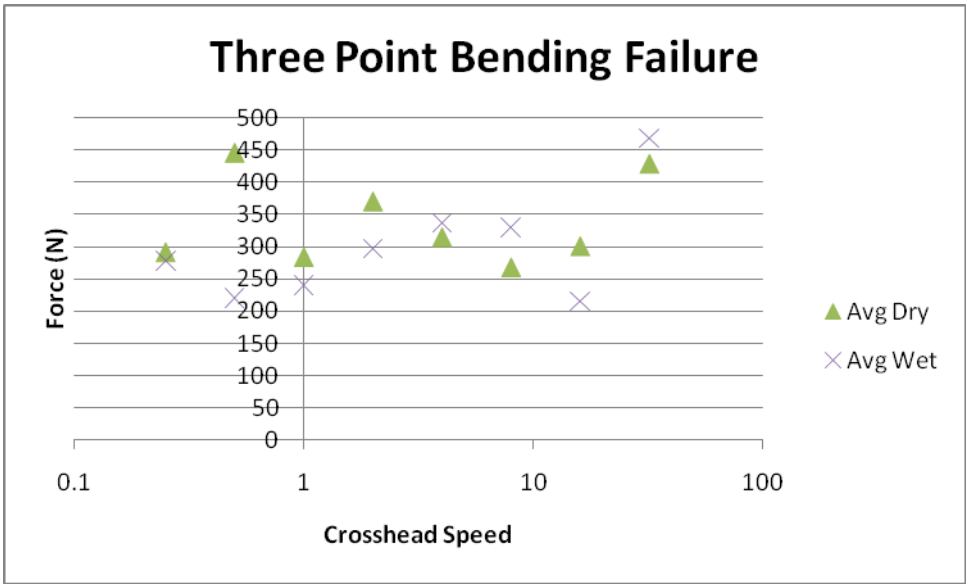

Figure 8. Failure force verses crosshead speed (untreated balsa)

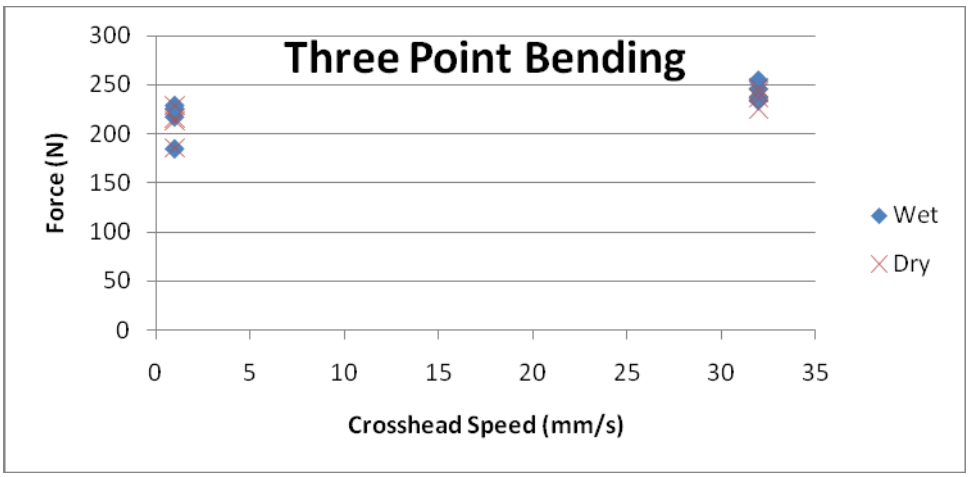

Figure 9. Medium has no effect of failure load but increasing strain rate increases ultimate strength. (hot coated balsa)

C. IMPACT TESTING

Contrary to the results seen in three-point bending with constant strain rate, impact with submergence in water had a significant effect on failure loads and also on modes of failure. As with the three-point bending tests, there was a fair amount of scatter, but some very significant trends can be observed. All impact testing was done on samples with ProBalsa Plus core.

An initial series of tests with a faulty force gage yielded a very interesting result. All dry samples except for one failed at the boundary with no damage at center span while the submerged samples mostly failed on centerline and sometimes with damage at boundary edges. This trend continued throughout testing. Table 5 summarizes the combined results of the initial test and progressive testing. Mid-span failures also showed secondary damage at the boundaries, but boundary failures did not have damage midspan.

Table 5. Failure locations

	Failure Location	
	Mid-span	Boundary
Wet	5	2
Dry	1	5

The next test series was a progressive test where a drop height was started at 355.6 mm (14 in) for two impacts, and then increased by 50.8 mm (2 in) for two more impacts, continuing in this pattern until the sample failed. Failure was determined by a significant loss of impact force on the second impact at the same height, visual damage, or an obvious failure on the force/time plot. The results of progressive testing are summarized in Table 6.

This progressive test data was used to design the next sequence of testing. Drop heights for single drop tests were intended to induce failure at the lowest possible velocity in both dry and submerged samples. Dry samples were tested at 660.4 mm (26 in) and submerged samples were tested at 457.2 mm (18 in). Table 7 was compiled from this data.

Table 6. Progressive impact data

Progressive Impact Testing Force Data 18 Oct

Drop Height (mm)	355.6	355.6	406.4	406.4	457.2	457.2	508	508	558.8	558.8	609.6	609.6	660.4	Damage Location
Dry 1	822.92	836.26	867.40	916.33	965.26	845.16	894.09	911.88	943.02	925.23	978.60	1000.85	1009.74	boundary
Dry 2	742.85	698.37	791.78	742.85	751.75	831.81	854.05	876.30	911.88	911.88	1031.98			boundary
Dry 3	Visable flaw at center span													
Dry 4	773.99	671.68	831.81											mid span
Wet 1	778.44	671.68	729.50	742.85	796.23	613.85	689.47	658.33						Mid span
Wet 2			920.78	969.71	916.33	925.23								boundary
Wet 3	805.12	805.12	889.64	849.61	885.19									mid span
Wet 4	902.98	929.67	1005.29	1054.22	1089.81									mid span

*Forces in Newtons. Shaded cells indicate failure

Table 7. Single drop impact data

Submerged Single Drop Impact Test

Test Date	Spec. Name	Drop Height	Max Force (N)	Comments	Failure Location	Failure Mode
1-Nov	18-1	457.2	947.47		boundary	skin compression
1-Nov	18-2	457.2	1054.22		boundary	skin compression
1-Nov	18-3	457.2	862.95		mid span	shear/ delam
1-Nov	18-4	457.2	782.88		mid span	skin compression
8-Nov	18-1	457.2	no data	strain gages	mid span	delam
8-Nov	18-2	457.2	995.00	strain gages	mid span	delam/shear/punch through
9-Nov	18-1	457.2	1075.68	questionable gage		no damage
9-Nov	18-2	457.2	1096.70	questionable gage	boundary	skin compression
1-Nov	26-1	660.4	1000.85		boundary	delam point flaw from sawing
1-Nov	26-2	660.4	1009.74		mid span	skin compression
		Wet average	**980.61**		**Mid span 5**	**Boundary 4**

Dry Single Drop Impact Test

Test Date	Spec. Name	Drop Height	Max Force (N)	Comments	Failure Location	Failure Mode
1-Nov	26-1	660.4	951.92		boundary	shear/delam
1-Nov	26-2	660.4	1103.15		boundary	skin compression/ shear
8-Nov	26-1	660.4	1042.92	strain gages	boundary/midspan	skin compression
9-Nov	22-1	558.8	928.60	questionable gage	boundary	light damage
9-Nov	24-1	609.6	1045.27	questionable gage	boundary	light damage
9-Nov	26-1	660.4	1383.23	questionable gage	boundary	skin compression
		Dry average	**1075.85**		**Mid span 1**	**Boundary 5**

The force/time graph of all dry failures show a high frequency response with an average period of 0.6 ms (Figure 10.) This frequency is observed on every test, regardless of damage. When failure can be seen on the plot, it typically occurred at the peak of the force plot with an abrupt drop in force as depicted in Figure 11.

Dry failure mode is dominated by skin failure in compression on the bottom of the beam at either boundary edge. Some samples also showed evidence of shear failure in the core at the same point such as the sample in Figure 12. Many samples had no evidence of any damage whatsoever at the mid span point of impact.

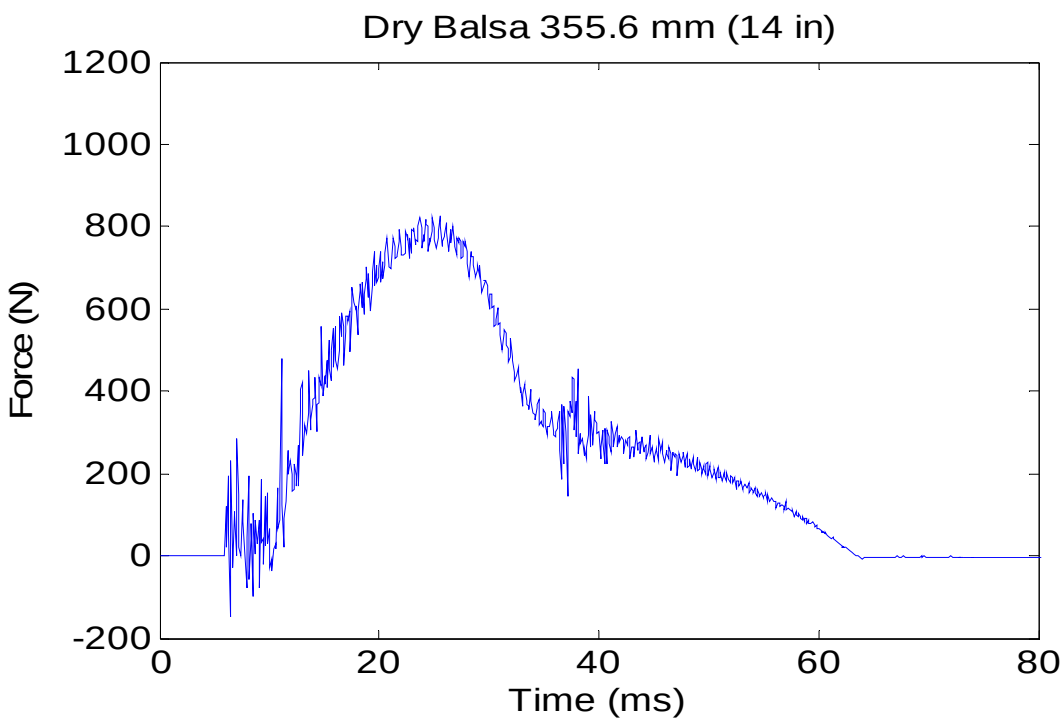

Figure 10. Dry Balsa with no damage

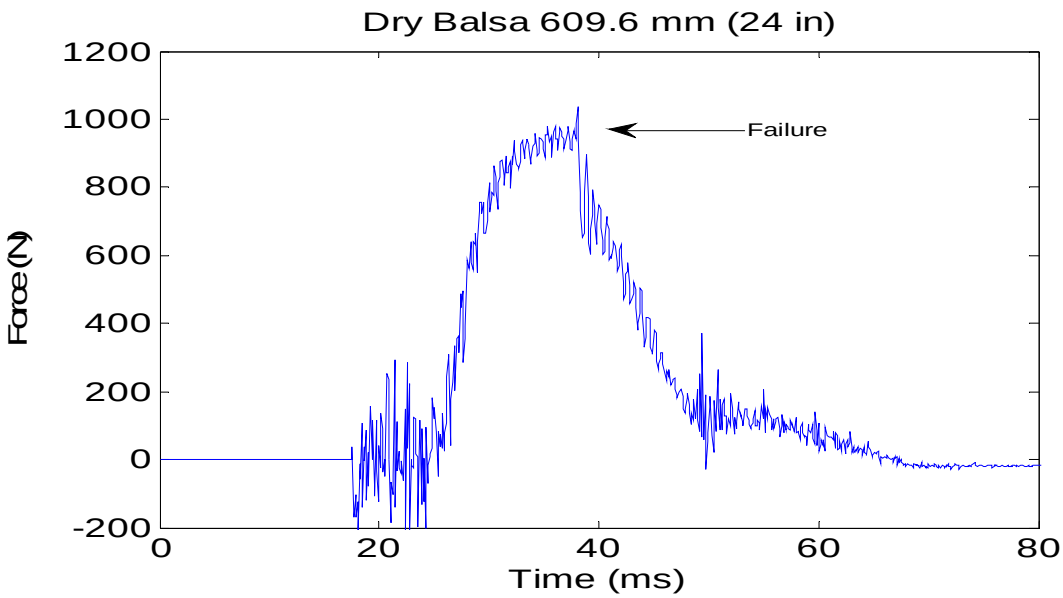

Figure 11. Dry Balsa Failure

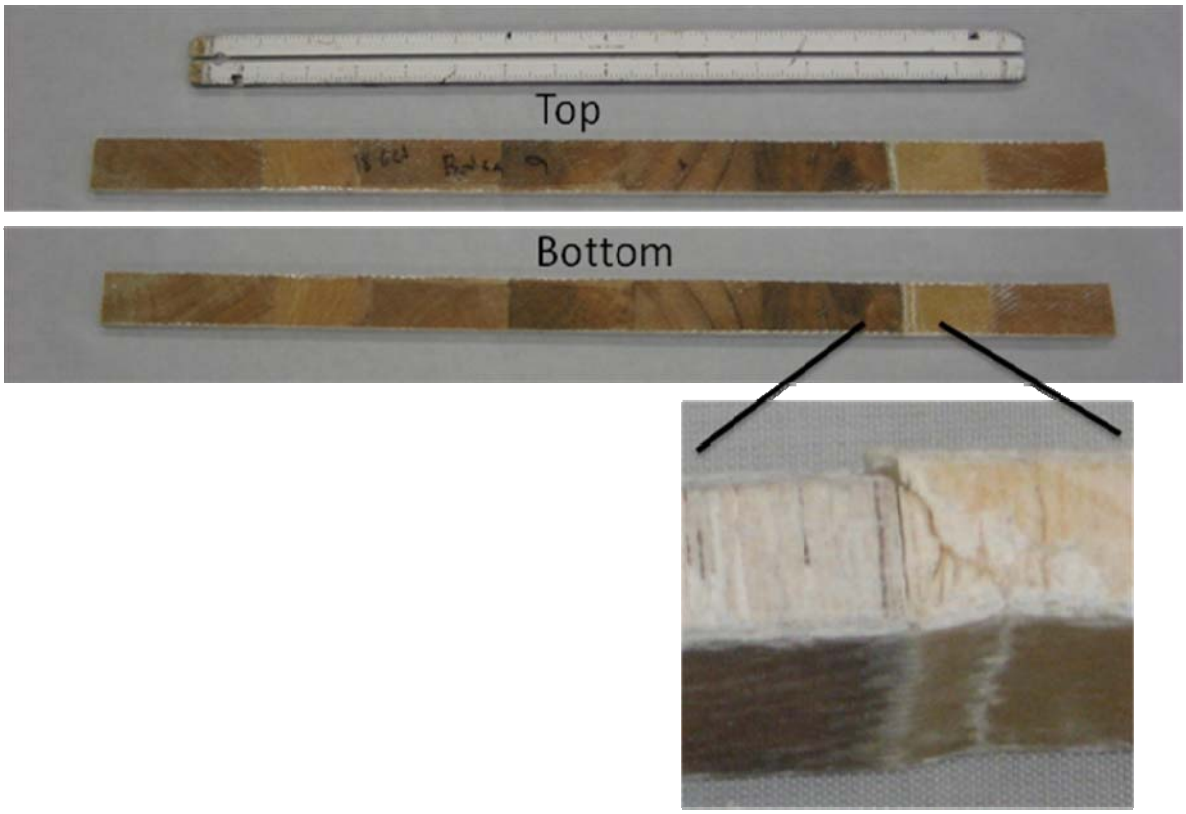

Figure 12. Dry impact damage with core shearing. The rightmost fracture line was right at the edged of the clamped boundary.

The force/time plots for submerged samples show a high frequency response with an average period of 0.6 ms similar to dry testing. However, the submerged samples also exhibited a secondary frequency response with an average period of 2.5 ms. This mode had greater applidute than the 0.6 ms mode and can easily be seen in Figures 13 and 14. Failure often occurred after the force had peaked (Figure 14.)

Submerged impact damage was primarily observed at centerspan with some damage also occuring at the edges of the beam. Failure mode was skin compression adjacent to the point of impact on the top skin with some localized delamination as seen in Figure 15. Any core damage at these sites was from bending, and did not show any sign of impact compression because the vertical cellular structure of the balsa was completely intact, but there was indication that the balsa had been compress longitudally, ie, across the grain. There was no evidence of water intrusion at any point. Submerged impact damage at one or both ends often appeared in the form of skin compression with out evidence of shear failure in the core.

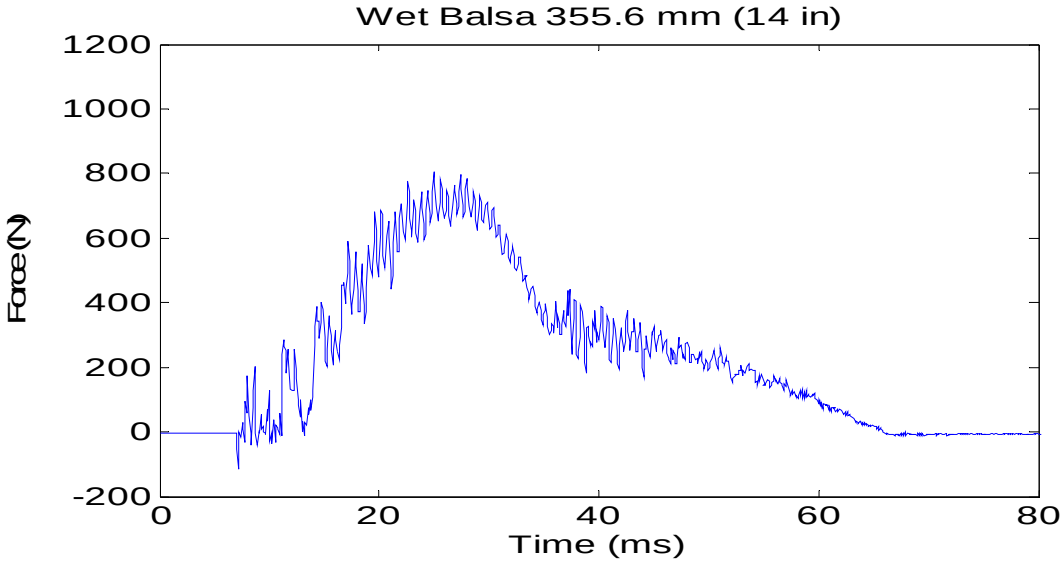

Figure 13. Submerged impact without failure

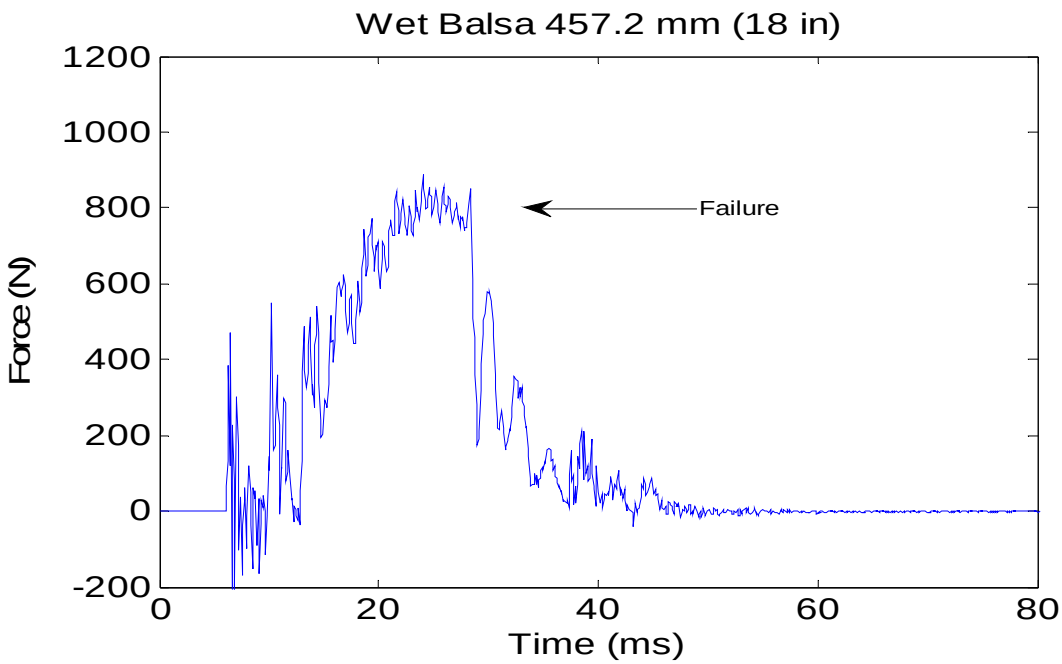

Figure 14. Submerge impact failure.

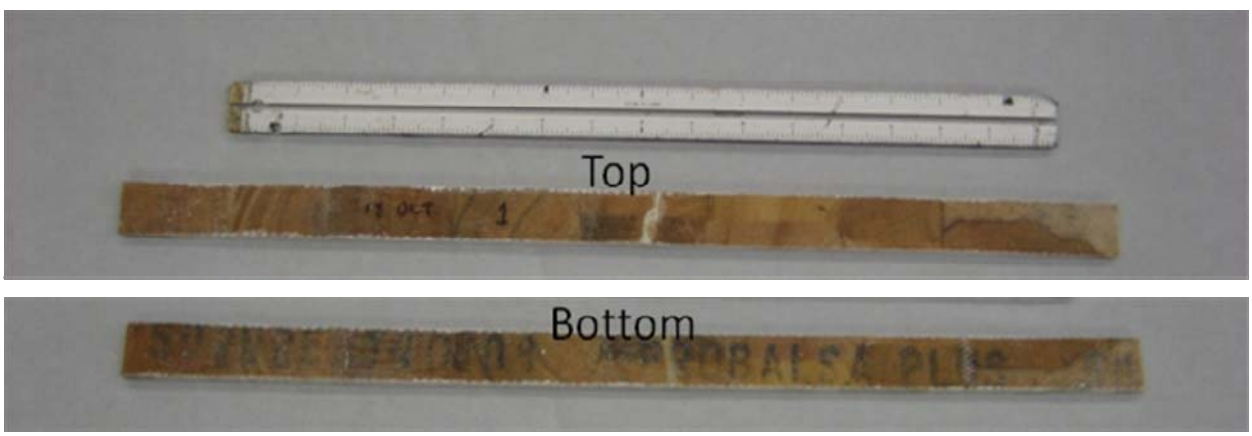

Figure 15. Typical submerged impact damage.

D. STRAIN DATA

In an effort to better understand the results, strain gages were included in the lay-up. Although an early feasibility test of this method had very promising results with no gage delamination and consistent data through multiple impacts, , no data was gathered from this current feasibility test. This embedded-strain-gage approach was attempted

again, but was not as successful, perhaps because the panel with the second batch of strain may have been opened prematurely. Despite some inconsistent data, the results are still worth examination (Figures 16, 17).

A third batch of strain gages was glued on using conventional techniques. These gages responded much like the other set, and, in fact, no centerline gages were able to last through the entire impact sequence or even up to peak force. This set appears to have increased in strength do to a more complete cure, and all samples were much stronger than the previous test one month prior even though they were cut from the same panel (Figures 18-21).

Figure 16 shows a dry impact which failed both on centerline and at the boundary opposite the boundary strain gage where 8.1 ms elapse from first strain response to peak strain. Figure 17 shows a submerged impact with failure on centerline. While the centerline strain gage follows the force profile, the amplitude is clearly not correct. Elapsed time from first strain response to peak strain was 11.9 ms. Figure 18 shows a submerged impact that did not fail. The centerline gage shows greater amplitude than the boundary gage, and is indicative of what is expected for a submerged impact. Figure 19 shows a submerged mid-span failure from a drop height of 609.6 mm (24 in). This drop was required to achieve failure as previously discussed. Figure 20 shows a submerged boundary failure. This plot indicates an early failure at the boundary followed by some residual strength in the rest of the beam. Figure 21 shows a combined failure from 762 m (30 in) drop height. This is an obvious outlier that took progressive impacts to achieve failure. This is the same sample from Figure 18.

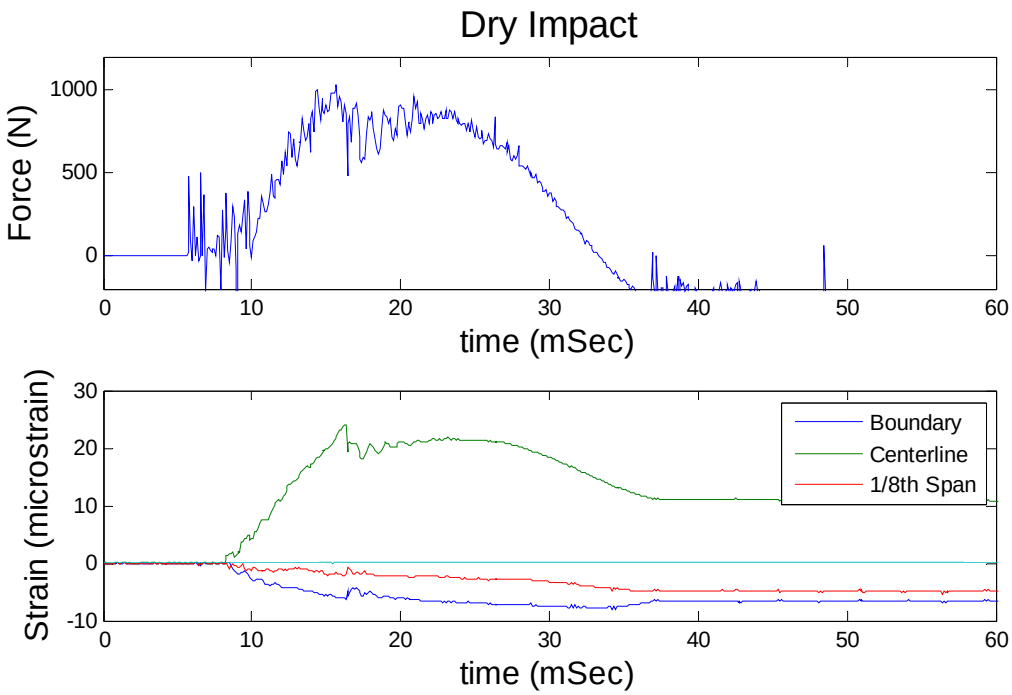

Figure 16. Dry impact, centerline and boundary failure

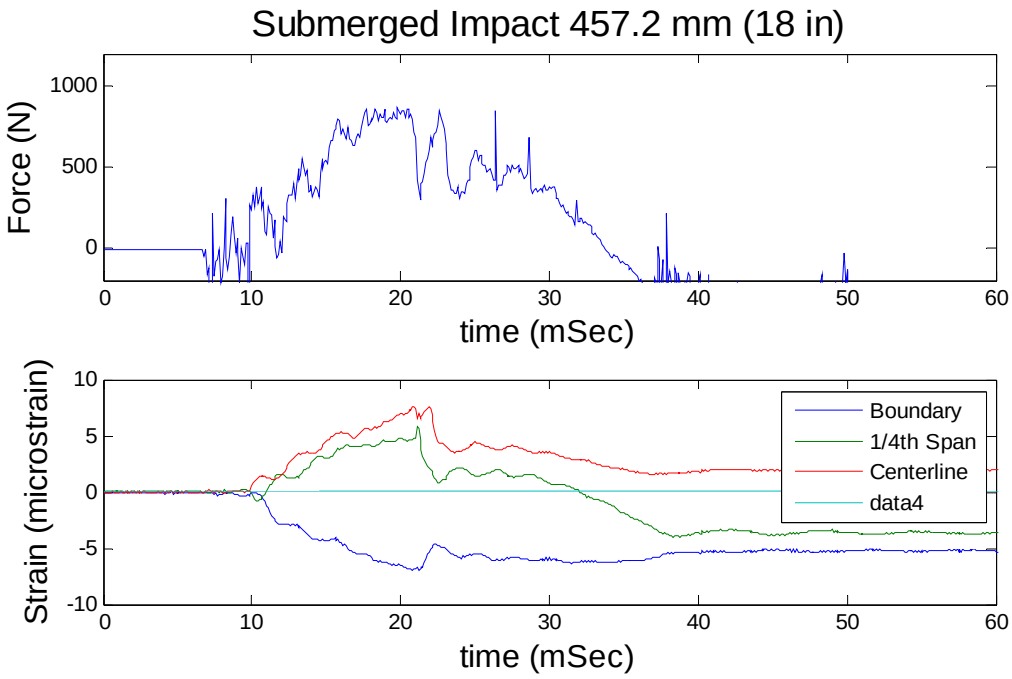

Figure 17. Submerged impact, centerline failure

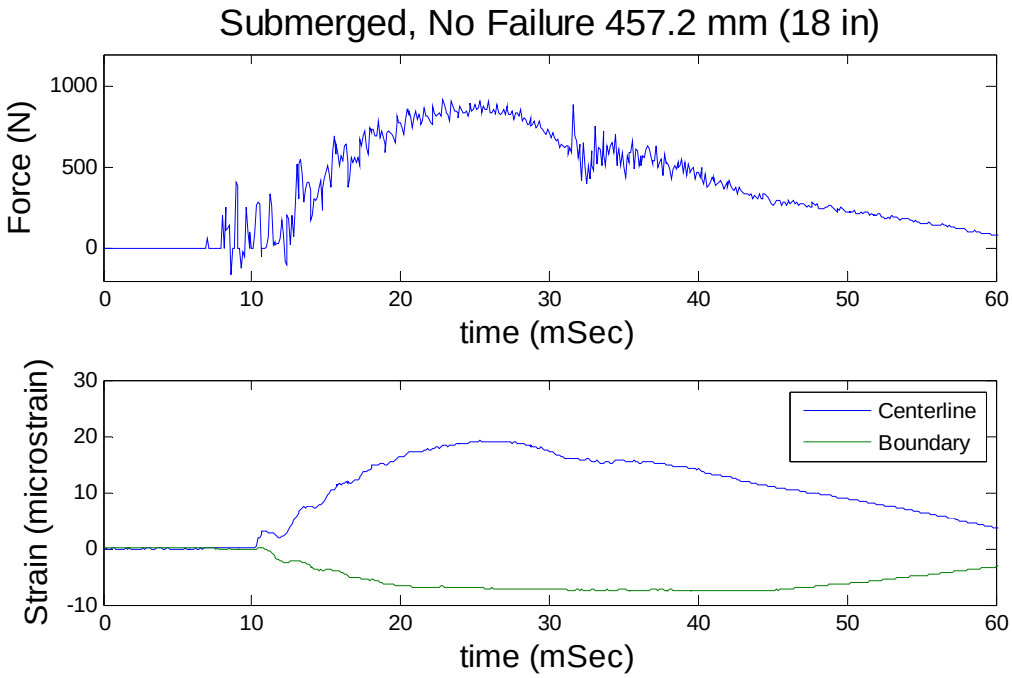

Figure 18. Submerged impact, no failure

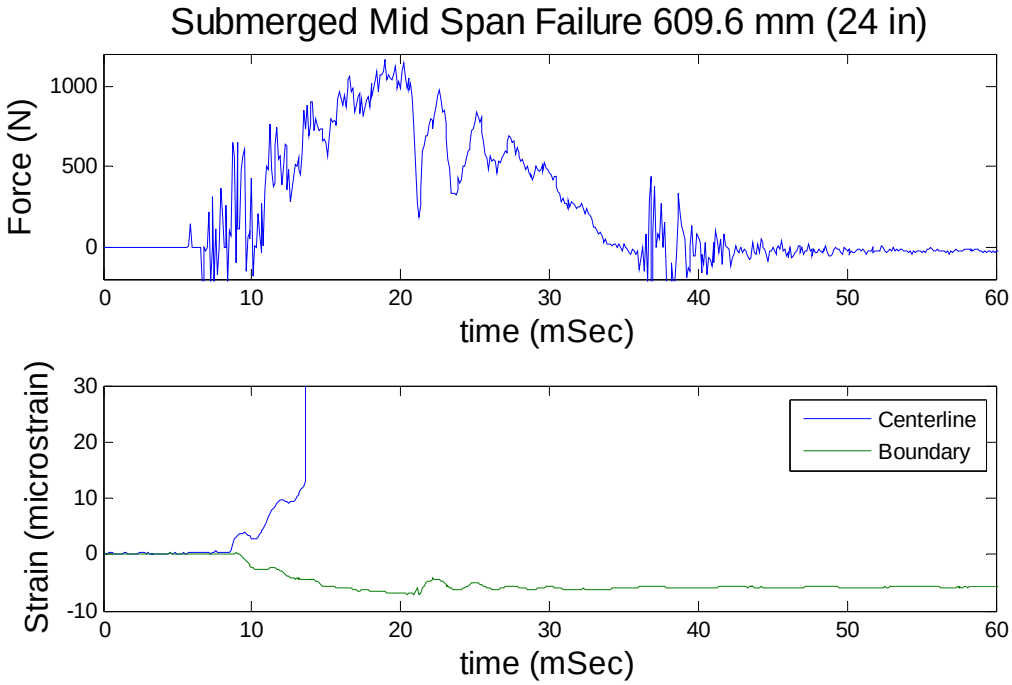

Figure 19. Submerged impact, mid-span failure

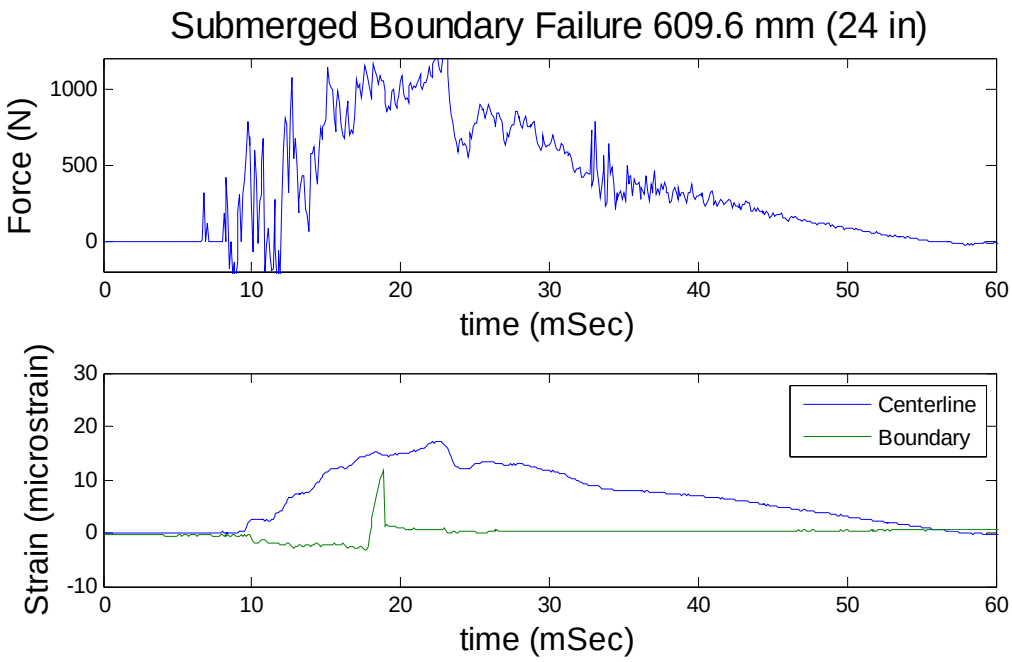

Figure 20. Submerged impact, boundary failure

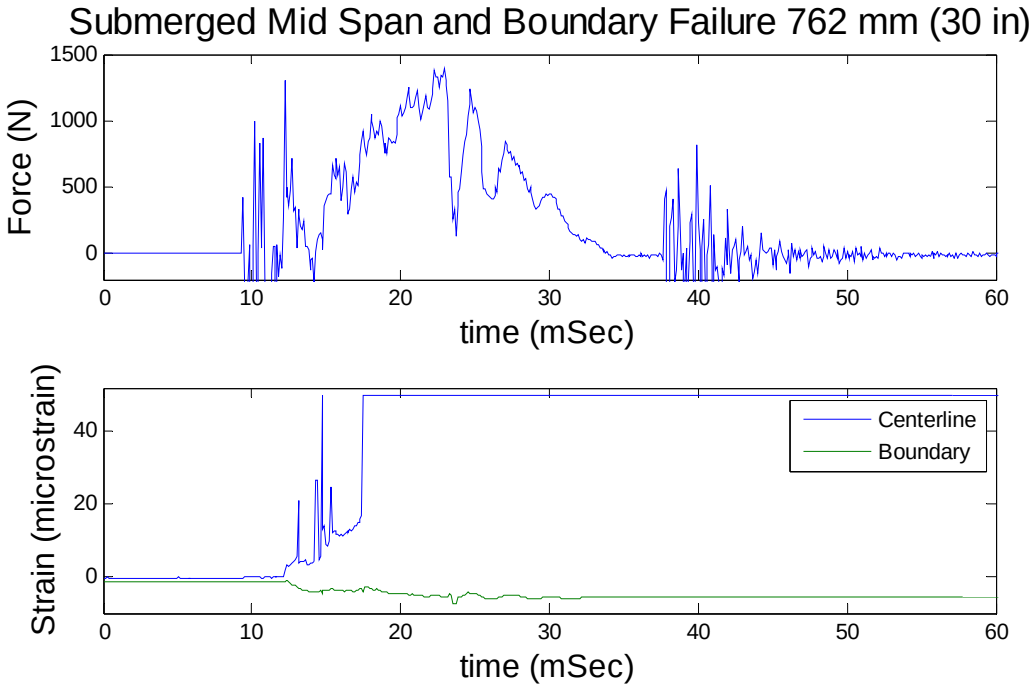

Figure 21. Submerged impact, boundary and mid-span failure

E. DISCUSSION

1. Failure Mode

Dry impact failure mode is dominated by skin failure in compression on the bottom of the beam at either edge. Some samples also showed evidence of shear failure in the core at the same point, while submerged impact damage was dominated by failures at center span. To understand this phenomenon, it is helpful to examine the shear and bending diagrams of each situation. With a downward point load at the center representing impact force, a beam in a clamped/clamped condition has the magnitude of the shear force is constant throughout the beam and the maximum bending moment is equal at center span and each edge. Assuming an upward uniform load distribution to represent the forces from the fluid structure interaction and then using superposition to combine the two curves shows a very interesting result. The graphs in Figures 22 and 23 were generated using a point load of -1000 N as seen is testing, and an assumed uniform load of 2.5 N/m to simulate the resistance imparted by the water as the sample accelerates under impact.

In the submerged samples, the absolute value of the bending moment decreases across the span but has a more significant effect on edges. The max bending moment is no longer shared by three points but instead found solely at center span. At the same time, the amount of shear force the sample experiences at the boundaries decreases significantly. Because failures are often mixed mode, and the clamped boundary condition creates a significant stress riser, the combination of max shear force and max bending moment at the edge of the dry beam seems very logical for failure at the edges. The reduction in both shear and bending moment at the edges for submerged samples also explains why submerged samples would be more likely to experience failure at center span.

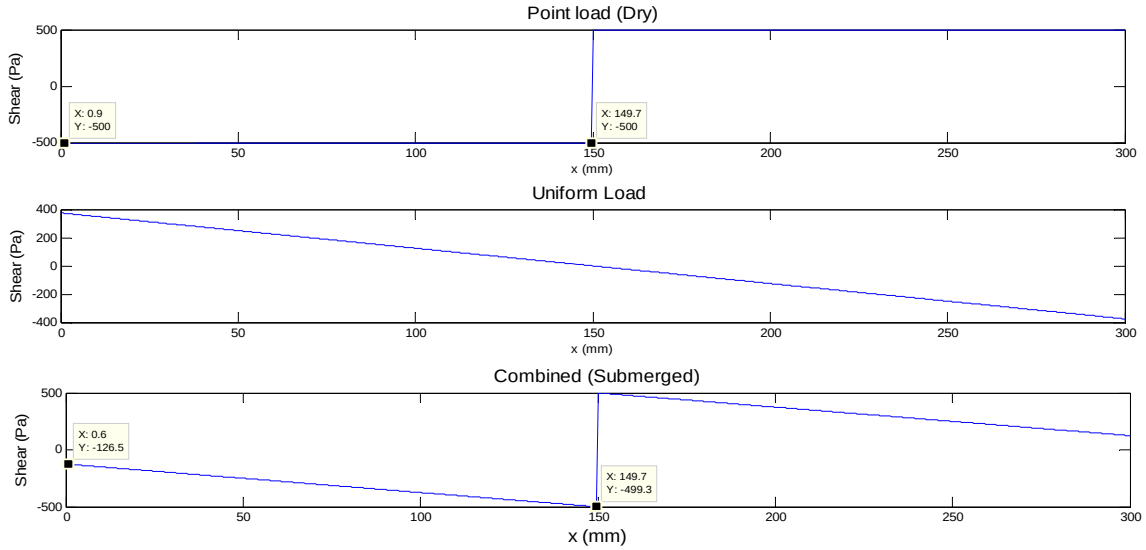

Figure 22. Shear force diagram

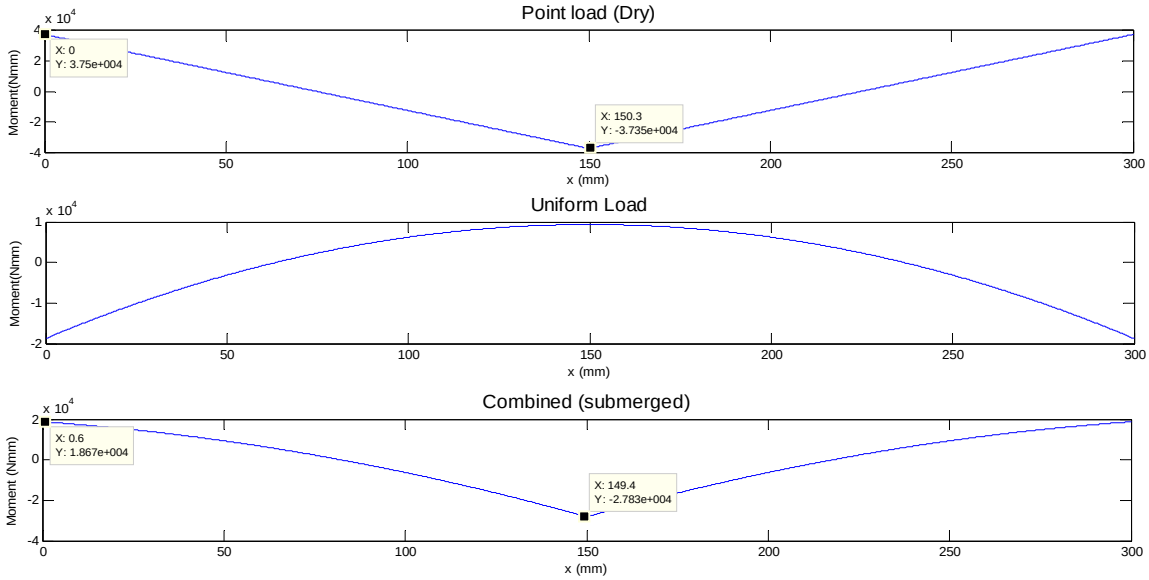

Figure 23. Bending moment diagram

2. Failure Loads and Drop Height

While it seems counterintuitive that submerged impact would impart more damage than a dry impact from equal height, this study clearly demonstrated that this was not the case. Progressive testing conclusively demonstrated that submerged samples require less drop height for failure. Three-point bending showed a good correlation

between strain rate and ultimate strength, and stain data from impact testing shows a higher strain rate for dry samples, which suggests that the difference in failure drop height is a matter of material characteristics varying with strain rate.

Additionally, when subjected to equal impact velocities, the submerged samples absorbed on average 7% more force than the dry samples due to the inertial effect of the fluid resisting acceleration (Table 8) of the beam structure. There is also an indication that the inertial force imparted by the fluid caused submerged beams continued to deflect after the peak impact force resulting in the failure after peak force as shown in figures 13 and 18.

Table 8. Average force for equal impact velocity

	Average Force (N)		
Drop Height (mm)	355.6	406.4	457.2
Dry	757.68	830.03	858.50
Wet	815.50	895.20	921.89
Difference	57.83	65.17	63.39
% Difference	7.09	7.28	6.88

IV. CONCLUSIONS AND RECOMMENDATIONS

In this study, a series of experiments was conducted to study the dynamic response of sandwich cored composite beams submerged in water subjected to a low velocity impact. Because the amount of data scatter and relatively limited number of testes conducted it is difficult to draw quantitative conclusion from this study. However, it is clearly seen that the added mass effect of fluid structure interaction has a significant influence on the mode of failure and effect of the impact force. Specifically, submerged beams in a clamped condition are more susceptible to mid span damage from bending at a lower impact velocity, while the same beam in a dry condition can withstand higher forces and is more likely to experience shear failure along the clamped boundaries. Submerged impact at the same velocity imparts approximately 7% more force than dry impact.

These results have serious implications for marine engineering and naval architecture as the need to define design margins and to predict failure becomes more important. Developing analytical methods for predicting added mass effect on composites, and investigating types of damage and damage thresholds for composites submerged in water and subjected to low velocity impact is paramount to refining the art and science of this field.

Future studies should include further investigation into strain response, investigation of different core materials and varying core thicknesses, and statistical analysis and modeling of balsa cored sandwich structures. To improve repeatability, a post cure bake needs to be incorporated into the sample production process.

THIS PAGE INTENTIONALLY LEFT BLANK

LIST OF REFERENCES

[1] DIAB Sandwich Handbook, DAIB AB, box 201, S-312 22, LAHOLM, Sweden, Sept 2003, http://www.diabgroup.com/europe/literature/e_pdf_files/man_pdf/sandwich_hb.pdf Accessed November 21, 2010

[2] Y. W. Kwon, A. C. Owens, A. S. Kwon, and J. M. Didoszak, "Experimental Study of Impact on Composite Plates with Fluid-Structure Interaction," Int. Journal of Multiphysics, vol. 4, no. 3, 2010, 259–271.

[3] A. P. Mouritz, E. Gellert, P. Burchill, K. Challis, Review of Advanced Composite Structures for Naval Ships and Submarines, Composite Structures, vol. 53, pp. 21–41, 2001.

[4] Z. Aslan, R. Karakuzu, B. Okutan, "The Response of Laminated Composite Plates Under Low-Velocity Impact Loading," Composites Structures, vol. 59, pp. 119–127, 2003.

[5] S. Abrate, "Impact on Laminated Composites; Recent Advances, "Applied Mechanics Reviews 47 pp. 517–544, November 1994.

[6] P. R. Hampson, M. Moatamedi, "Fluid Structure Interaction of Submerged Metallic and Composite Plates Subjected to Low Velocity Impact Loading," International Journal of Crash Worthiness, vol. 15, 49–58.

[7] K. S. Tan, "Dynamic Loading Characteristics in Metals and Composites," M.S. Thesis, Mech. Eng., Naval Postgraduate School, Monterey, Ca. December 2009.

[8] A. E. Armenakas, C. A. Sciammarella, "Response of Glass-Fiber-Reinforced Epoxy Specimens to High Rates of Tensile Loading," *Experimental Mechanics*, vol. 13, no. 10, pp. 433–440, October 1973.

[9] J. M. Lifshitz, "Impact strength of angle ply fiber reinforced materials," *Journal of Composite Materials*, vol. 10, pp. 92–101, January 1976.

[10] O. I. Okoli, and G. F. Smith, "The effect of strain rate and fibre content on the Poisson's ratio of glass/epoxy composites," *Composite Structures*, vol. 48, pp. 157–161, January 2000.

[11] N. Taniguchi, T. Nishiwaki, N. Hirayama, H. Nishida, H. Kawada, "Dynamic tensile properties of carbon fiber composite based on thermoplastic epoxy resin loaded in matrix-dominated directions," *Composites Science and Technology*, vol. 69, pp. 207–213, February 2009.

[11] M. M. Shokrieh, and M. J. Omidi, "Tension behavior of unidirectional glass/epoxy composites under different strain rates," *Composite Structures*, vol. 88, pp. 595–601, March 2009.

[12] I. M. Daniel, R. H. LaBedz, and T. Liber, "New method for testing composites at very high strain rates," *Experimental Mechanics*, vol. 21, no. 2, pp. 71–77, February 1981.

[13] J. Harding, and L. M. Welsh, "A tensile testing technique for fibre-reinforced composites at impact rates of strain," *Journal of Materials Science*, vol. 18, pp. 1810–1826, June 1983.

[14] O. I. Okoli, and G. F. Smith, "The effect of strain rate and fibre content on the Poisson's ratio of glass/epoxy composites," *Composite Structures*, vol. 48, pp. 157–161, January 2000.

[15] A. C. Owens, "An Experimental Study of Fluid Structure interaction of Carbon Composites under Low Velocity Impact," M.S. Thesis, Mech. Eng., Naval Postgraduate School, Monterey, Ca. December 2009.

[16] ProBals Technical Manual, DAIB AB, box 201, S-312 22, LAHOLM, Sweden, September 2003, http://www.diabgroup.com/europe/literature/e_pdf_files/man_pdf/Probalsa_Man.pdf Accessed November 23, 2010.

[17] Standard Guide for Testing Polymer Matrix Composite Materials, ASTM, D 4762 – 08, 2008.

[18] Francois Barthelat and Hubert Lobo, "High Velocity 3 Point Bending Test Using an Impact Tower," Datapoint Testing Services, Ithaca NY http://www.testpaks.com/3POINTBENDING.htm, Accessed November 23, 2010.

INITIAL DISTRIBUTION LIST

1. Defense Technical Information Center
   Ft. Belvoir, Virginia

2. Dudley Knox Library
   Naval Postgraduate School
   Monterey, California

3. Professor Young Kwon
   Naval Postgraduate School
   Monterey, California

4. Research Assistant Professor Jarema M. Didoszak
   Naval Postgraduate School
   Monterey, California

5. Douglas C. Loup
   Naval Surface Warfare Center, Carderock Division
   West Bethesda, Maryland

6. Erik A. Rasmussen
   Naval Surface Warfare Center Carderock Division
   West Bethesda, Maryland

7. Scott W. Bartlett
   Naval Surface Warfare Center Carderock Division
   West Bethesda, Maryland

8. Engineering and Technology Circular Office, Code 34
   Naval Postgraduate School
   Monterey, California

9. Ryan D. McCrillis
   Naval Postgraduate School
   Monterey, California